Supplemental Information

Brown adipose tissue controls skeletal muscle function via the secretion of myostatin

Xingxing Kong, Ting Yao, Peng Zhou, Lawrence Kazak, Danielle Tenen, Anna Lyubetskaya, Brian A. Dawes, Linus Tsai, Barbara B. Kahn, Bruce M. Spiegelman, Tiemin Liu, and Evan D. Rosen

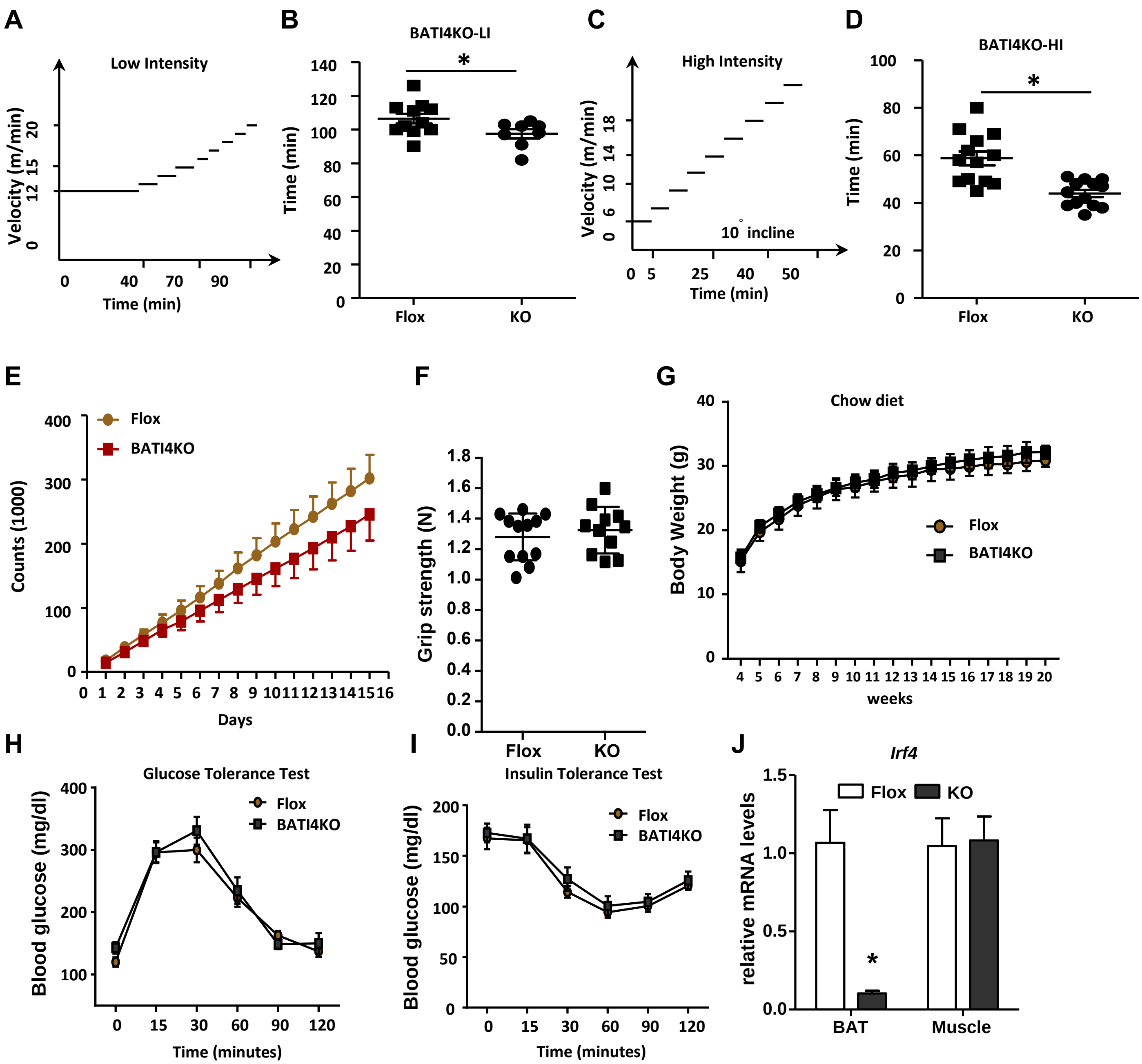

Figure S1: (Related to Figure 1)

Reduced exercise capacity in BATI4KO mice. (**A**) Schematic of low intensity and (**C**) high intensity exercise regimens. Time run by BATI4KO and control mice on low intensity (**B**) and high intensity (**D**) protocols. (**E**) Cumulative free wheel running in BATI4KO and control mice (n=8 per group). (**F**) Grip strength of BATI4KO groups mice. (**G**) Body weight of BATI4KO and Flox mice on chow diet. (n=9-16/group). (**H**) Glucose tolerance test in 12-week-old BATI4KO mice on chow diet after intraperitoneal injection of glucose. (n = 8). (**I**) Insulin tolerance test in 14-week-old BATI4KO mice after intraperitoneal injection of insulin. (n=8). (**J**) Q-PCR gene expression analysis of *Irf4* expression in BAT and vastus lateralis of BATI4KO mice. Results are expressed as mean ± SEM (n=5-6, *$p<0.05$).

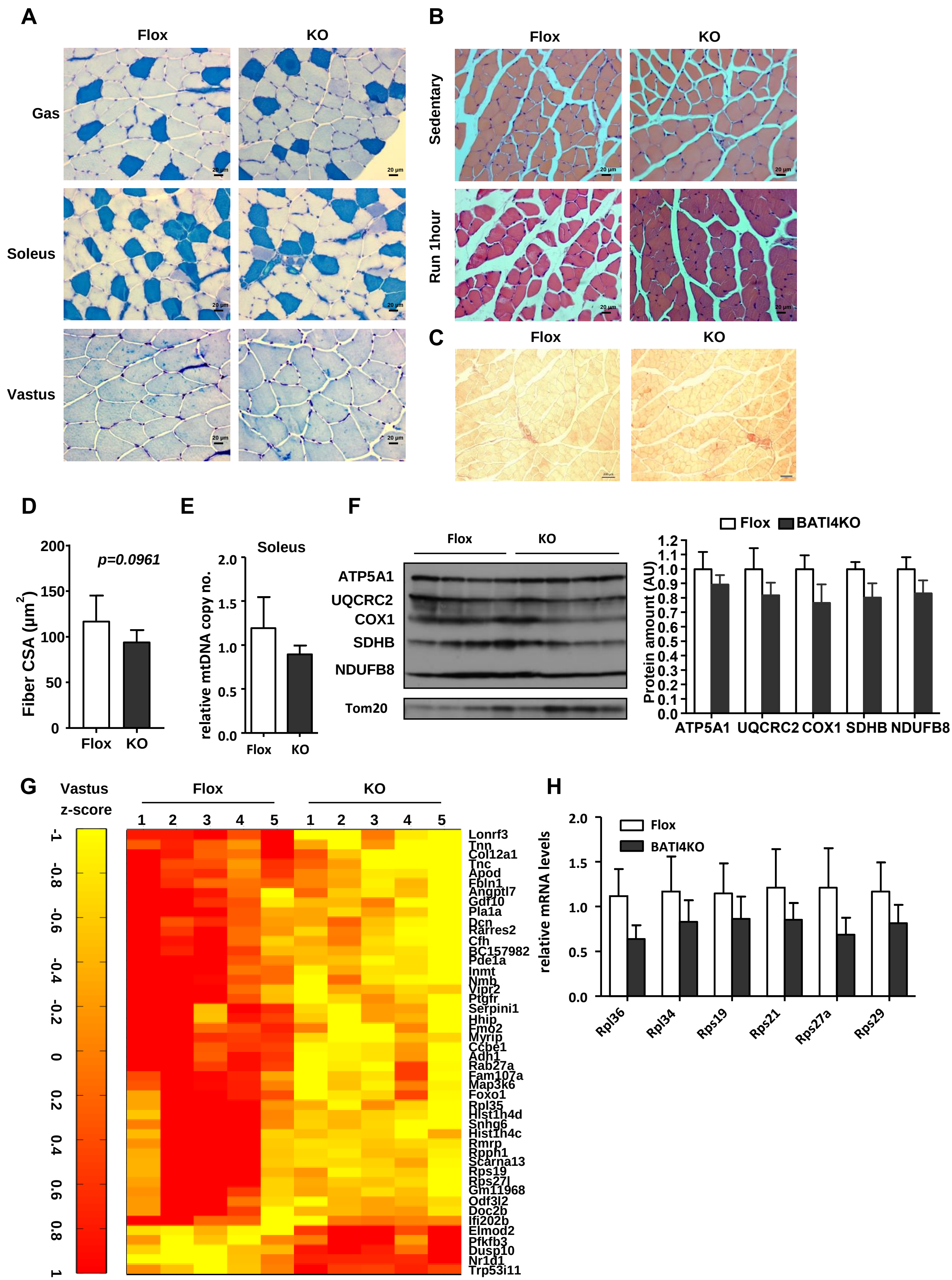
A
Flox
KO
Gas
Soleus
Vastus
B
Flox
KO
Sedentary
Run 1hour
C
Flox
KO
D
p=0.0961
Fiber CSA (μm2)
Flox
KO
E
Soleus
relative mtDNA copy no.
Flox
KO
F
Flox
KO
ATP5A1
UQCRC2
COX1
SDHB
NDUFB8
Tom20
Flox
BATI4KO
Protein amount (AU)
ATP5A1
UQCRC2
COX1
SDHB
NDUFB8
G
Vastus
z-score
Flox
KO
Lonrf3
Tnn
Col12a1
Tnc
Apod
Fbln1
Angptl7
Gdf10
Pla1a
Dcn
Rarres2
Cfh
BC157982
Pde1a
Inmt
Nmb
Vipr2
Ptgfr
Serpini1
Hhip
Fmo2
Myrip
Ccbe1
Adh1
Rab27a
Fam107a
Map3k6
Foxo1
Rpl35
Hist1h4d
Snhg6
Hist1h4c
Rmrp
Rpph1
Scarna13
Rps19
Rps27l
Gm11968
Odf3l2
Doc2b
Ifi202b
Elmod2
Pfkfb3
Dusp10
Nr1d1
Trp53i11
H
Flox
BATI4KO
relative mRNA levels
Rpl36
Rpl34
Rps19
Rps21
Rps27a
Rps29

Figure S2: (Related to Figure 2)

BATI4KO mice have altered skeletal muscle. (**A**) ATPase staining of muscle sections from BATI4KO and control mice (type I: dark blue; type IIa: white; type IIb: light blue). (**B**) H&E staining of soleus muscle from BATI4KO and control mice (40X). (**C**) Sirius Red staining of vastus muscle from BATI4KO and control mice (10X). (**D**) Muscle fiber cross-sectional area. Values are means ± SEM. (**E**) Mitochondrial DNA number in soleus muscle of BATI4KO and control mice (n=5). (**F**) Western blot analysis of isolated muscle mitochondria from soleus of BATI4KO and control mice. Protein amount was quantified using Image J. (n=4). (**G**) Heat map from RNA-seq of vastus lateralis from BATI4KO and control mice, $|\log2FC|>=1$, FDR $\leq$ 0.05. (**H**) Q-PCR analysis of ribosomal protein gene mRNA expression in the vastus (n=8-10).

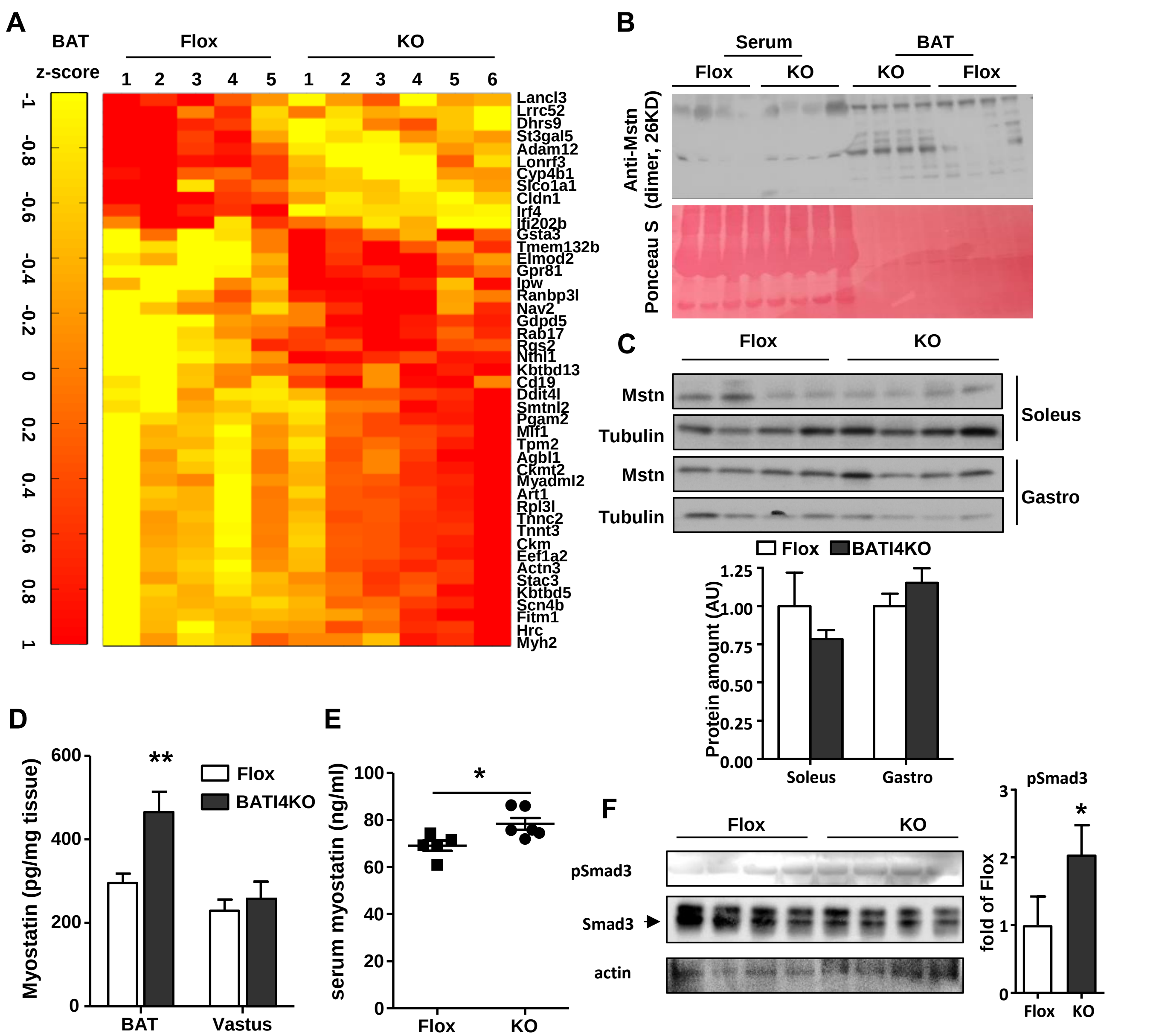

Figure S3: (Related to Figure 3)

Direct effect of BAT via secretion of myostatin. (**A**) Heat map of differentially expressed genes in BAT of BATI4KO and control mice, |log2FC|>=1, FDR ≤ 0.05. (**B, C**) Western blot analysis of muscle myostatin levels. Protein amount was quantified using Image J. (n=4). Tissue myostatin levels (**D**) and serum myostatin levels in BATI4KO group (**E**) were measured by ELISA kits. (n=5-8, **p*<0.05). (**F**) Western blot analysis of Smad3 phosphorylation in vastus of male BATI4KO vs. control mice. Activity was quantified using Image J (n=4, **p* < 0.05 vs. Flox mice).

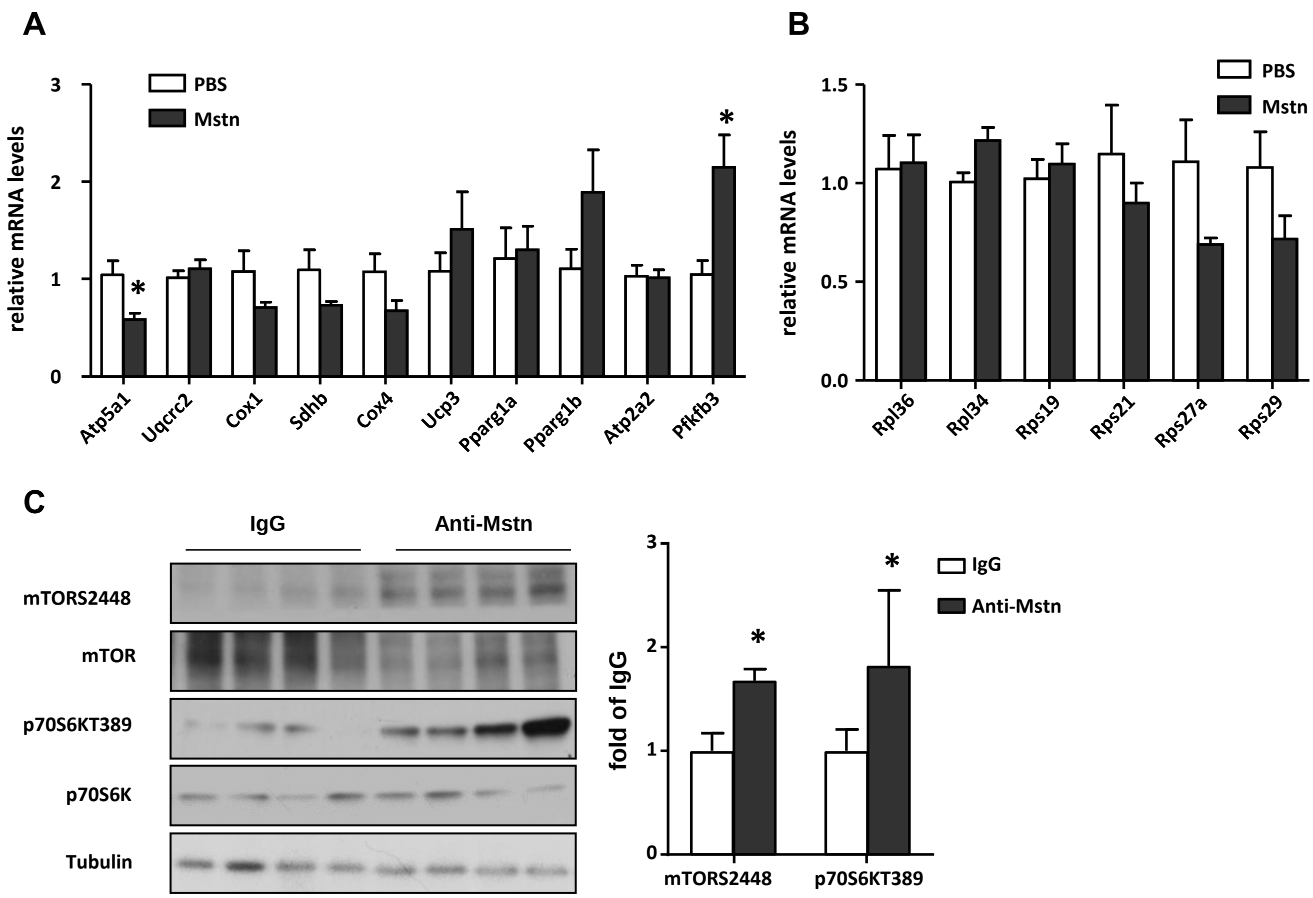

Figure S4: (Related to Figure 5)

Myostatin mediates the effect of BAT IRF4 loss on exercise capacity. Q-PCR analysis of mitochondrial gene expression (**A**) and ribosomal protein gene mRNA expression (**B**) in the vastus from myostatin injection groups (n=5-6, *$p < 0.05$). (**C**) Western blot analysis of mTOR signaling pathway in vastus lateralis of myostatin antibody injection groups. Activity was quantified using Image J (n=4, *$p < 0.05$ vs. IgG).

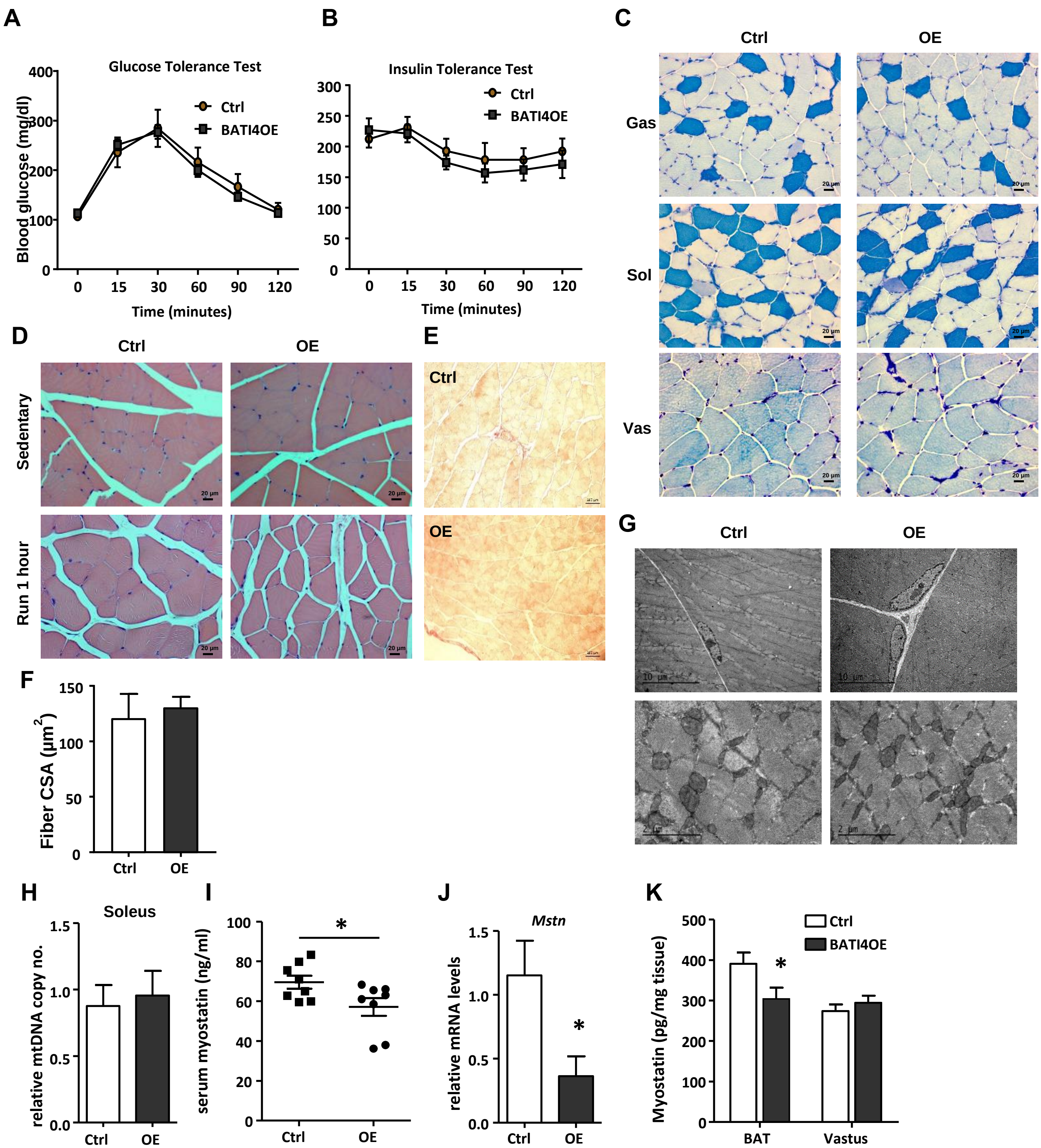

Figure S5: (Related to Figure 6)

Increased exercise capacity following myostatin neutralization or IRF4 overexpression. (**A**) Glucose tolerance test in 12-week-old BATI4OE mice on chow diet after intraperitoneal injection of glucose (n = 8). (**B**) Insulin tolerance test in 14-week-old BATI4OE mice after intraperitoneal injection of insulin (n=8). (**C**) ATPase staining of muscle sections from BATI4OE and control mice (type I: dark blue; type IIa: white; type IIb: light blue). (**D**) H&E staining of vastus lateralis from BATI4OE vs. control mice (40X). (**E**) Sirius Red staining of vastus muscle from BATI4KO and control mice (10X). (**F**) Muscle fiber cross-sectional area. Values are means ± SEM. (**G**) Electron micrograph of vastus lateralis from BATI4OE and control mice. (**H**) Mitochondrial DNA number in soleus of BATI4OE and control mice (n=4, 5). Serum myostatin levels (**I**) and tissue myostatin levels (**K**) in BATI4OE group were measured by ELISA kits (n=8, *$p<0.05$). (**J**) Q-PCR analysis of *Mstn* mRNA expression in BAT (n=5-6, *$p<0.05$) of BATI4OE and control mice.

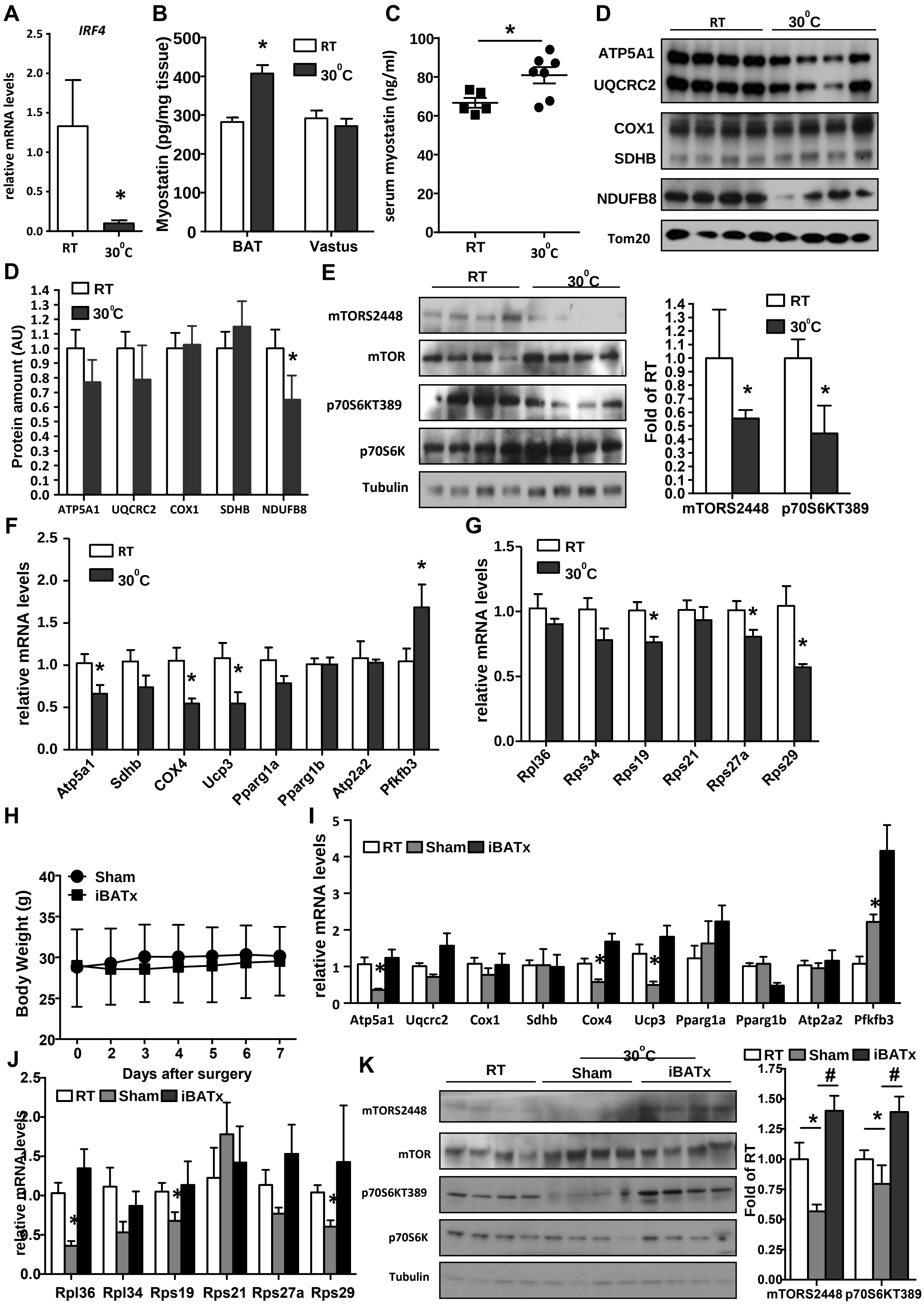
A
IRF4
relative mRNA levels
RT
30°C
B
Myostatin (pg/mg tissue)
RT
30°C
BAT
Vastus
C
serum myostatin (ng/ml)
RT
30°C
D
RT
30°C
ATP5A1
UQCRC2
COX1
SDHB
NDUFB8
Tom20
D
Protein amount (AU)
ATP5A1
UQCRC2
COX1
SDHB
NDUFB8
E
mTORS2448
mTOR
p70S6KT389
p70S6K
Tubulin
Fold of RT
F
relative mRNA levels
Atp5a1
Sdhb
COX4
Ucp3
Ppargc1a
Ppargc1b
Atp2a2
Pfkfb3
G
Rpl36
Rps34
Rps19
Rps21
Rps27a
Rps29
H
Sham
iBATx
Body Weight (g)
Days after surgery
I
RT
Sham
iBATx
Atp5a1
Uqcrc2
Cox1
Sdhb
Cox4
Ucp3
Ppargc1a
Ppargc1b
Atp2a2
Pfkfb3
J
Rpl36
Rpl34
Rps19
Rps21
Rps27a
Rps29
K
Sham
iBATx
mTORS2448
mTOR
p70S6KT389
p70S6K
Tubulin
Fold of RT
mTORS2448
p70S6KT389

Figure S6: (Related to Figure 7)

Warming causes myostatin elevation and myopathy in a BAT-dependent manner. (A) *Irf4* mRNA levels in BAT from mice at RT and 30ºC. Tissue myostatin levels (**B**) and serum myostatin levels (**C**) were measured by ELISA kits. (n=5-8, $*p<0.05$). (**D**) Western blot analysis of isolated mitochondria from vastus of WT mice at RT and 30°C. Protein amount was quantified using Image J (n=4, $*p < 0.05$ vs. RT mice). (**E**) Western blot analysis of mTOR signaling pathway in vastus of WT mice at RT and 30°C. Activity was quantified using Image J. (n=4, $*p < 0.05$ vs. RT mice). (**F**) Q-PCR analysis of vastus gene expression (n=5-6, $*p < 0.05$). **(G)** Q-PCR analysis of vastus ribosomal gene expression (n=5-6, $*p < 0.05$). **(H)** Body weight (BW) of iBATx and sham-operated mice after surgery. **(I)** Q-PCR analysis of vastus gene expression before and after iBATx and exposure to 30°C (n=5-6, $*p < 0.05$). **(J)** Q-PCR analysis of vastus ribosomal gene expression before and after iBATx and exposure to 30°C (n=5-6, $*p < 0.05$). **(K)** Western blot analysis of mTOR signaling pathway in vastus from mice before and after iBATx and exposure to 30°C. Activity was quantified using Image J (n=4, $*p < 0.05$ vs. Flox mice. $\#p < 0.05$ vs. iBATx mice).

Table S3: (Related to STAR Methods) Primers used for qRT-PCR

Gene	Forward	Reverse
Atp2a2	GAGAACGCTCACACAAAGACC	CAATTCGTTGGAGCCCCAT
Pfkfb3	CCCAGAGCCGGGTACAGAA	GGGGAGTTGGTCAGCTTCG
Irf4	CAGGACTACAATCGTGAGGAGG	GCACATCGTAATCTTGTCTTCCA
Atp5a1	TCTCCATGCCTCTAACACTCG	CCAGGTCAACAGACGTGTCAG
Uqcrc2	AAAGTTGCCCCGAAGGTTAAA	GAGCATAGTTTTCCAGAGAAGCA
COX1	GGATTTGTTCACTGATTCCCATTA	GCATCTGGGTAGTCTGAGTAGCG
SDHB	AATTTGCCATTTACCGATGGGA	AGCATCCAACACCATAGGTCC
COX4	GTTCAGTTGTACCGCATCCA	TTGTCATAGTCCCACTTGGC
UCP3	TTTCTGCGTCTGGGAGCTT	GGCCCTCTTCAGTTGCTCAT
Pparg1a	GGACATGTGCAGCCAAGACTCT	CACTTCAATCCACCCAGAAAGCT
Pparg1b	GGCAGGTTCAACCCCGA	CTTGCTAACATCACAGAGGATATCTTG
Rpl36	ATGGTCAACGTACCAAAAACCC	TGGGCATACAGGGAATCCTTG
Rpl34	TCGGTGGCCCTATTGAGTG	GCTCGGCTGATACTCGTTTCC
Rps19	GCCTCCCAGGCTCTGAAAC	GCTTTGAGGTGGTCTCGACA
Rps21	GTCCATCCAGATGAACGTGG	CCATCAGCCTTAGCCAATCGG
Rps27a	GACCCTTACGGGGAAAACCAT	AGACAAAGTCCGGCCATCTTC
Rps29	GTCTGATCCGCAAATACGGG	AGCCTATGTCCTTCGCGTACT
Mstn	AGTGGATCTAAATGAGGGCAGT	GTTTCCAGGCGCAGCTTAC
Actn3	AACAGCAGCGGAAAACCTTCA	GGCTTTATTGACATTGGCGATTT
Asb18	GACTCGCCCCCAGATTACC	TCAGTGCAGATCAGCTTCTGTA
Cacng6	AGAACAGCAGAATCTCGGCTT	CCTGCCACAGTCGCTTGAT
Myod1	CCACTCCGGGACATAGACTTG	AAAAGCGCAGGTCTGGTGAG
Myh8	AACAGAAACGCAATGCTGAGG	TCGCCTGTAATTTGTCCACCA
Tnnt1	CCTGTGGTGCCTCCTTTGATT	TGCGGTCTTTTAGTGCAATGAG
TBP	CCCCTTGTACCCTTCACCAAT	GAAGCTGCGGTACAATTCCAG
36B4	GAGGAATCAGATGAGGATATGGGA	AAGCAGGCTGACTTGGTTGC